ELSEVIER

July 1994

Materials Letters 20 (1994) 183–187

MATERIALS LETTERS

On the reversible and athermal photo-vitrification phenomenon of $As_{50}Se_{50}$ chalcogenide thin films

E. Márquez, C. Corrales, J.B. Ramírez-Malo, J. Reyes, J. Fernández-Peña, P. Villares, R. Jiménez-Garay

Departamento de Estructura y Propiedades de los Materiales, Facultad de Ciencias, Universidad de Cádiz, Apdo. 40, 11510 Puerto Real (Cádiz), Spain

Received 4 April 1994; accepted 11 April 1994

Abstract

This work reports the first optical study of a novel amorphization process, namely photo-induced vitrification, in a chalcogenide material, $As_{50}Se_{50}$. The phenomenon is reversible and athermal, in the sense that local melting is thought not to be involved, but the process does appear to be thermally activated with an activation energy of 0.15 eV. On the other hand, the analysis proposed by Swanepoel, enabling the determination of the thickness variation, average thickness and refractive index of a wedge-shaped film has successfully been applied. The refractive-index behaviour of the as-evaporated, crystallized and photo-vitrified $As_{50}Se_{50}$ films under study is analyzed within the oscillator framework proposed by Wemple and DiDomenico.

Light-induced structural changes in amorphous As-chalcogenide materials have been known for a long time [1]. Reversible changes are only observed in well-annealed amorphous thin films or bulk glasses where they can be removed by annealing near the glass transition temperature, T_g [2,3]. It has also been reported that illumination with high-intensity light can lead to photo-crystallization of $GeSe_2$ [4]. In this Letter we report on a new study of a novel photo-induced structural effect in amorphous chalcogenide materials, namely the athermal light-induced vitrification of $As_{50}Se_{50}$ thin films [5,6]. The first optical analysis of this phenomenon presented here, is based on a very appealing method proposed by Swanepoel [7], which takes into consideration the lack of thickness uniformity of the thermally evaporated chalcogenide glass films.

The bulk starting material was prepared by direct synthesis from 5 N purity elements heated together in an evacuated quartz ampoule at about 950°C for 24 h. After the synthesis the melt was air-quenched, resulting in a bulk glass of the required chemical composition. X-ray diffraction (XRD) analysis showed that the ingot was amorphous. On the other hand, the studied thin-film samples were prepared by thermal evaporation of the $As_{50}Se_{50}$ bulk glass onto room-temperature glass substrates in a vacuum of $\approx 10^{-6}$ Torr using a conventional coating unit (Edwards, model E306A). During evaporation the substrates were rotated (≈ 45 rpm) in order to obtain an enhanced degree of film thickness uniformity [8] – the variation in thickness over the area under study, measured by a stylus-based surface profiler (Sloan Technology Corporation, model Dektak IIA), was found to be lower than 40 nm. Electron microprobe analysis of the as-deposited $As_{50}Se_{50}$ thin films indicated that the stated composition was correct to $\pm 0.5\%$. The deposition rate was approximately 10 Å s^{-1}, and this quantity was continuously measured by a quartz crystal monitor (Edwards, model FTM-5).

0167-577x/94/$07.00 © 1994 Elsevier Science B.V. All rights reserved
SSDI 0167-577x(94)00099-9

The film thicknesses were in the range 700–1200 nm. The samples were annealed at 150°C (T_g=164°C) for periods of, typically, 72 h in a $\approx 10^{-3}$ Torr vacuum. Illumination of the glass films was carried out using a 500 W high-pressure mercury lamp (Oriel, model 66041), through an IR-cut filter, providing broadband white light (with a very high UV output).

The optical transmission spectra used in the present study were obtained over the 300–2000 nm spectral region by a double-beam UV/VIS/NIR computer-controlled spectrophotometer (Perkin-Elmer, model Lambda-19). The spectrophotometer was set with a slit width of 1 nm. It was therefore unnecessary to make slit width corrections, since that value of the slit width was much smaller than the different linewidths. The area of illumination over which a single transmission spectrum was obtained was about 1 mm×10 mm. All the optical constant measurements reported in this Letter were made at room temperature.

The XRD pattern (using Cu Kα radiation) of an as-evaporated $As_{50}Se_{50}$ film is shown in Fig. 1 and it indicates that the film is amorphous. It should be noted that one aspect of the diffraction results on chalcogenide materials has been ascribed to the influence of medium-range order, and this is the so-called first sharp diffraction peak (FSDP) or prepeak in the structure factor [9,10]. This peak almost invariably occurs at a value of the modulus of the scattering vector of ≈ 1 Å^{-1} in amorphous chalcogenides. Furthermore, it is well known that most chalcogenide glasses are rather resistant to crystallization (particularly binary As-chalcogenides). Nevertheless, the $As_{50}Se_{50}$ film samples could be crystallized by annealing, and comparison of the XRD pattern of the crystallized film with powder-diffraction data for As–Se binary crystals taken from Ref. [11] enables us to unambiguously identify the crystalline phase of the film as c-As_4Se_4 (the corresponding crystal system is monoclinic). However, it should be mentioned that the peak intensities differed somewhat from the reference powder-diffraction data, indicating possible preferred orientational effects in the crystallized films. Also worth noting is the virtual absence of FSDP at $2\theta \approx 17°$, characteristic of the amorphous phase, in the crystallized product.

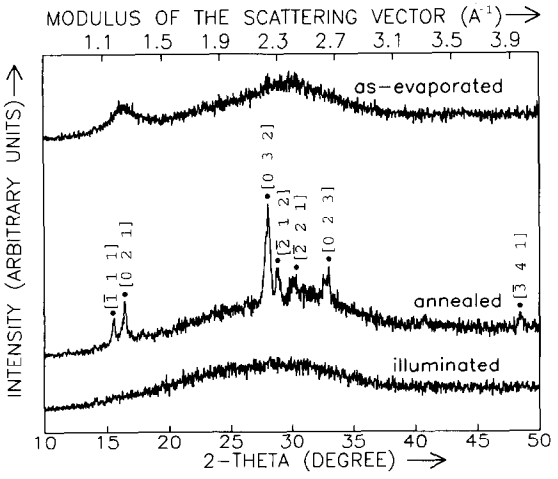

Fig. 1. X-ray diffraction patterns (Cu Kα radiation) of the as-evaporated, crystallized and photo-vitrified $As_{50}Se_{50}$ thin films, respectively, on a glass substrate.

Next, exposure of the crystallized $As_{50}Se_{50}$ film to white light from the mercury arc lamp (intensity ≈ 300 mW cm^{-2}) for 10 h at room temperature caused the complete disappearance of the crystalline features in the XRD pattern, i.e. the $As_{50}Se_{50}$ film was photo-amorphized. The temperature increase of the film during the illumination process, as measured by a thermocouple conveniently affixed to the surface of the glass film, was never more than 25°C (interestingly, this temperature increase represents an advantage because, considering that the photo-vitrification process was found to be thermally activated [5], ΔE=0.15 eV, the illumination time necessary to vitrify the film is reduced by 35%), indicating that the light-induced amorphous-state transformation under this low-intensity condition is effectively athermal. One differentiating structural characteristic of the photovitrification process which takes place using white light from a mercury lamp, in relation to that which takes place when a quartz tungsten halogen lamp is used (Elliott and Kolobov used this kind of light source when they first observed the phenomenon [5,6]) is the total disappearance of FSDP in the former, while in the latter there is practically no difference between the XRD patterns of as-evaporated and photo-vitrified films.

Moreover, the crystallization–vitrification process was found to be reversible; the photo-vitrified film could again be crystallized by thermal annealing at 150°C and subsequently vitrified once more by illumination. This reversible effect can be repeated many

times; for instance, we have performed five such cycles on one of our samples. It should be emphasized that this unusual photo-induced effect seems to be unique to $As_{50}Se_{50}$ films: our attempts to crystallize other amorphous As–Se films with different composition by annealing them for 72 h, as the prelude to investigating the photo-vitrification phenomenon, have clearly failed.

The calculation procedures of the refractive index, n, and average film thickness, $\bar{d}$, will now be presented. First of all, the optical transmission, $T_{\Delta d}$, in the transparent region at a specific wavelength λ, for the present case of non-uniform thickness, can be obtained by the expression [7]

$$T_{\Delta d} = \frac{1}{\varphi_2 - \varphi_1} \int_{\varphi_1}^{\varphi_2} \frac{A}{B - C\cos\varphi + D}\, d\varphi , \qquad (1)$$

where $A = 16n^2 s$, $B = (n+1)^3(n+s^2)$, $C = 2(n^2-1)(n^2-s^2)$, $D = (n-1)^3(n-s^2)$, $\varphi = 4\pi nd/\lambda$, with $\varphi_1 = 4\pi n(\bar{d} - \Delta d)/\lambda$ and $\varphi_2 = 4\pi n(\bar{d} + \Delta d)/\lambda$. It is assumed that the thickness varies linearly over the illuminated area, so that the thickness is: $d = \bar{d} \pm \Delta d$ (see Fig. 2). Δd refers to the actual variation in thickness from the average thickness and s is the refractive index of the substrate. The expressions for the envelopes around the interference maxima and minima of the optical transmission spectrum are the following [7]:

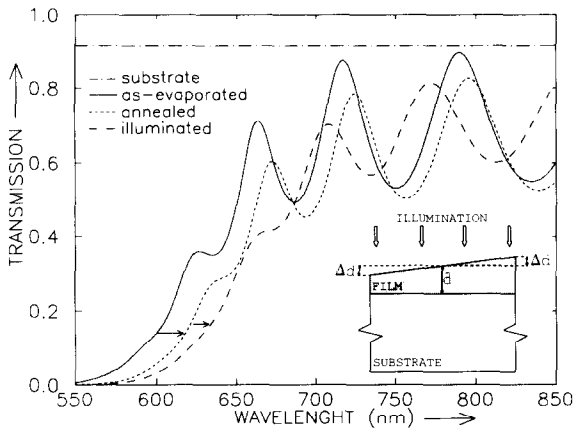

Fig. 2. Typical optical transmission spectra for the as-deposited, crystallized and photo-amorphized $As_{50}Se_{50}$ thin films, respectively. Also, diagram showing an absorbing thin film with a linear variation in thickness on a thick transparent substrate.

$$T_{\max} = \frac{2a}{\Delta\varphi(1-b^2)^{1/2}} \tan^{-1}\left[\frac{1+b}{(1-b^2)^{1/2}} \tan\left(\frac{\Delta\varphi}{2}\right)\right],$$

$$T_{\min} = \frac{2a}{\Delta\varphi(1-b^2)^{1/2}} \tan^{-1}\left[\frac{1-b}{(1-b^2)^{1/2}} \tan\left(\frac{\Delta\varphi}{2}\right)\right], \qquad (2)$$

where $a = A/(B+D)$, $b = C/(B+D)$ and $\Delta\varphi = \varphi_2 - \varphi_1$. The range of validity of Eq. (2) is: $0 < \Delta d < \lambda/4n$. In addition, the two expressions included in Eq. (2) are two independent transcendental equations with only two unknown parameters, n and Δd. They have been successfully solved for the experimental values using a standard computer method (Newton–Raphson iteration).

On the other hand, Fig. 2 shows three typical transmission spectra corresponding to the as-evaporated, crystallized and photo-vitrified $As_{50}Se_{50}$ films, respectively. Firstly, the values of the maximum and minimum transmission, $T_{\max}$ and $T_{\min}$, are used in Eq. (2) to derive the values of the refractive index and thickness variation, shown as n_1 and Δd in Table 1 (some of the results belonging to the photo-amorphized film are presented as a representative example). From the very stable values of Δd in Table 1 it seems reasonable to suggest a value for the thickness variation of ≈ 34 nm. In addition, the values of n_1 can be used to derive $\bar{d}$ from the basic equation for the interference fringes, $2n\bar{d} = m\lambda$ (m is the order number of the interference extrema), and also improved values for n, shown as n_2, as described in detail in our previous work [13]. If this is carried out, the value of $\bar{d}$ obtained in this particular case is 1109 ± 19 nm (the accuracy is 1.7%). The values of the thickness variation and average film thickness for the as-evaporated and crystallized $As_{50}Se_{50}$ films are given in Table 2. The values of the inhomogeneity parameter Δd show that the film quality decreases (it becomes more wedge-shaped) as it is subjected to the different treatments. As to the $\bar{d}$ values, a densification process takes place first, and a photo-induced volume expansion follows.

Next, the spectral dependence of the refractive index is fitted to the Wemple–DiDomenico dispersion relationship [14], that is, the single-oscillator model

Table 1
Values of λ, T_{max} and T_{min} for the photo-vitrified $As_{50}Se_{50}$ transmission spectrum shown in Fig. 2; the underlined transmittance values are those derived by the envelope computer program [12]. Also, the accuracy improvement procedure for the refractive indices n_1

λ (nm)	s	T_{max}	T_{min}	n_1	Δd (nm)	m	n_2
1435	1.519	0.895	0.590	2.615	32.8	4.0	2.588
1283	1.532	0.888	0.594	2.614	32.4	4.5	2.603
1163	1.542	0.880	0.597	2.624	32.4	5.0	2.622
1066	1.543	0.872	0.598	2.633	33.4	5.5	2.643
984	1.538	0.863	0.602	2.636	34.7	6.0	2.662
918	1.533	0.854	0.604	2.645	35.5	6.5	2.690
860	1.532	0.844	0.603	2.668	35.9	7.0	2.714
813	1.525	0.831	0.602	2.698	36.7	7.5	2.749

Table 2
Values of the thickness variation Δd, average thickness $\bar{d}$, dispersion parameters E_o and E_d (single-oscillator analysis) and optical band gap E_g^{opt} (Tauc's extrapolation) for the thin films under study

Sample	$\bar{d}$ (nm)	Δd (nm)	E_o (eV)	E_d (eV)	E_g^{opt} (eV)
as-evaporated	1119±10(0.9%)	18	4.07	24.08	1.87
crystallized	1066±11(1.1%)	28	3.92	25.86	1.81
photo-vitrified	1109±19(1.7%)	34	3.64	19.56	1.78

$$\epsilon_1(E) = n^2(E) = 1 + \frac{E_o E_d}{E_o^2 - E^2}, \qquad (3)$$

where E_o is the single-oscillator energy (typically near the main peak of the $\epsilon_2(E)$-spectrum) and E_d is the dispersion energy. By plotting $(n^2-1)^{-1}$ against E^2 and fitting a straight line as shown in Fig. 3, E_o and E_d are determined directly from the slope, $(E_o E_d)^{-1}$, and the intercept, E_o/E_d, on the vertical axis. The values of the dispersion parameters E_o and E_d for the as-evaporated, crystallized and photo-vitrified films are listed in Table 2. The tendency of E_o is such that it is verified that $E_o \approx 2E_g^{opt}$ (see Table 2) [15], whereas E_d according to Wemple and DiDomenico [14] obeys the proportionality relation $E_d \propto N_c^e$, N_c^e being in this particular case the effective As coordination number, which implies that, indeed, gross structural changes are inherent to the process of athermal photo-amorphization of $As_{50}Se_{50}$ thin films.

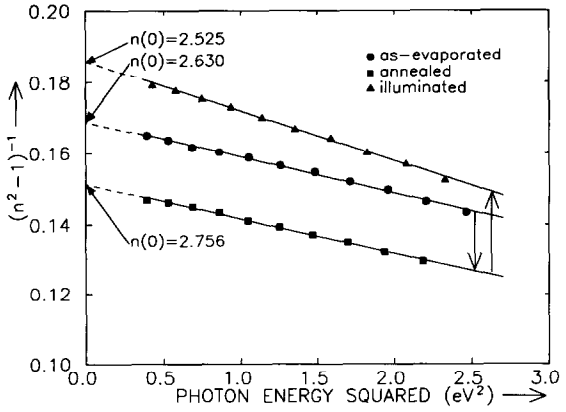

Fig. 3. Plot of the refractive-index factor $(n^2-1)^{-1}$ versus E^2 for the as-deposited, crystallized and photo-vitrified films, respectively; $n(0)$ values are the refractive indices extrapolated to $E=0$.

Finally, the crystal structure of $As_{50}Se_{50}$ is composed of As_4Se_4 quasi-spherical molecules, i.e. it is a molecular crystal. Illumination conceivably causes intramolecular bond breaking of covalent bonds within the As_4Se_4 molecules, giving rise to an amorphous cross-linked network. Alternatively, photo-induced intermolecular bond breaking of van der Waals or weak covalent bonds between As_4Se_4 molecules could occur, resulting in a translationally and orientationally disordered amorphous phase in which the integrity of the As_4Se_4 molecules is preserved. A more detailed study of the photo-induced amorphization phenomenon is currently under way and the results will be published elsewhere.

The authors would like to acknowledge some very useful discussions with A.V. Kolobov and R. Swanepoel.

References

[1] J.S. Berkes, S.W. Ing and W. Hillegas, J. Appl. Phys. 42 (1971) 4908.
[2] Ke. Tanaka, Rev. Solid State Sci. 4 (1990) 641.
[3] G. Pfeiffer, M.A. Paesler and S.C. Agarval, J. Non-Crys. Solids 130 (1991) 111.
[4] J.E. Griffiths, G.P. Espinosa, J.P. Remeika and J.C. Phyllips, Phys. Rev. B 25 (1982) 1272.
[5] S.R. Elliott and A.V. Kolobov, J. Non-Crys. Solids 128 (1991) 216.
[6] A.V. Kolobov, V.A. Bershtein and S.R. Elliott, J. Non-Crys. Solids 150 (1992) 116.
[7] R. Swanepoel, J. Phys. E 17 (1984) 896.
[8] K.H. Behrndt, in: Physics of thin films, eds. G. Hass and R.E. Thun (Academic Press, New York, 1964) p. 46.
[9] S.C. Moss and D.L. Price, in: Physics of disordered materials, eds. D. Adler, H. Fritzsche and S.R. Ovshinsky (Plenum Press, New York, 1985) p. 77.
[10] S.R. Elliott, Phys. Rev. Letters 67 (1991) 711.
[11] Powder Diffraction File, Inorganic Phases, JCPDS International Centre for Diffraction Data, 1988.
[12] M. McClain, A. Feldman, D. Kahamer and X. Ying, Comp. Phys. 5 (1990) 45.
[13] E. Márquez, J. Ramírez-Malo, P. Villares, R. Jiménez-Garay, P.J.S. Ewen and A.E. Owen, J. Phys. D 25 (1992) 535.
[14] S.H. Wemple and DiDomenico, Phys. Rev. B 7 (1973) 3767.
[15] J. Ramírez-Malo, E. Márquez, P. Villares and R. Jiménez-Garay, Phys. Stat. Sol. 133a (1992) 499.